Saudi Journal of Biological Sciences 28 (2021) 901–910

Contents lists available at ScienceDirect

Saudi Journal of Biological Sciences

journal homepage: www.sciencedirect.com

Original article

Cellulase immobilized magnetic nanoparticles for green energy production from *Allamanda schottii* L: Sustainability research in waste recycling

Shankar Vijayalakshmi [a], Marimuthu Govindarajan [b,c], Norah Al-Mulahim [d], Zubair Ahmed [d], Shahid Mahboob [d,*]

[a] CO_2 Research and Green Technologies centre, VIT University, Vellore 632014, India
[b] Department of Zoology, Annamalai University, Annamalainagar 608 002, Tamil Nadu, India
[c] Unit of Natural Products and Nanotechnology, Department of Zoology, Government College for Women (Autonomous), Kumbakonam 612 001, Tamil Nadu, India
[d] Department of Zoology, College of Science, King Saud University, Riyadh, 11451, Saudi Arabia

ARTICLE INFO

Article history:
Received 19 October 2020
Revised 5 November 2020
Accepted 8 November 2020
Available online 13 November 2020

Keywords:
Saccharomyces cerevisiae
Fermentation
Bioethanol
Immobilization
Biofuel
Allamanda schottii

ABSTRACT

This study presents ethanol's fabrication by fermenting the golden trumpet flower (*Allamanda schottii L*) with the yeast strain *Saccharomyces cerevisiae*. The changes in different parameters during fermentation were studied and optimized while producing the ethanol and the end product was subjected to emission test study by blending petrol and ethanol. The *Allamanda* floral substrate contains 65% polysaccharides. The strain *S. cerevisiae* was obtained in the form of baker's yeast from a domestic shop. For 100 ml of slurry, the highest bioethanol yield recorded was about 18.75 ml via optimization of different culture conditions, including a 1:8 ratio for slurry preparation, maintained under 35 ^{0}C, 5.5 pH, 72 h. old inoculum with a quantity of 3.75 g 100 ml^{-1}, fermented for120 h. The highest yield of bioethanol was acquired under the addition of urea. This technique & design is capable of industrial-scale fabrication of bioethanol by using *A. schottii* floral substrates. This research was conducted to fabricate ethanol by fermentation (*A. schottii* L*)* floral substrate with *S. cerevisiae.* The optimum physiochemical parameters required to obtain the highest yield of bioethanol from *A. schottii* flower by fermentation was studied. The immobilization strategy with a cheap agricultural substrate and magnetic nanoparticles were also studied. The engine performance and emission studies were done with different blends of petrol and bio-ethanol.

1. Introduction

Biomass energy reduces GHG emissions on a large scale. The CO_2 released on burning biomass is equal to fossil fuels (Kongkiattikajorn and Sornvoraweat, 2011). However, during photosynthesis, the CO_2 is captured for the growth of biomass and hence a balance exists. The biomass can be grown on underutilized farmland (Rankovic et al., 2009). Biofuels are the only renewable liquid transportation fuels that can reduce dependence on foreign oil. Huge biomass potential is available in our country to produce biodiesel and bioethanol, so investing in this sector proves to be economical (Raita et al., 2016). When burnt, the biomass can pollute the air, but at low levels than fossil fuels' burning. The Sulphur content, which causes acid rain, are not produced while burning the biomass. The burnt biomass releases CO_2, contributing to GHG emission but compensated by the photosynthesis process during biomass growth (Liu et al., 2018).

The first-generation biofuels are obtained from sugary, starchy and fatty food crops. Molasses, the byproduct of the sugar industry, are used to produce ethanol (Talebnia et al., 2010). The 2nd generation biofuels are mainly from lignocellulosic materials. The raw materials like wood, straw, agricultural, horticultural residues and forest waste are available in large quantities (Mittal, 1992). Various methods are available to convert these residues into biofuels. This type of biomass focuses mainly on avoiding food crop resources, which pose a threat to food security (Abdel Ghany et al., 2014). The second-generation processes mainly aim to

* Corresponding author at: Department of Zoology, College of Science, King Saud University, Riyadh, 11451, Saudi Arabia.
E-mail address: mushahid@ksu.edu.sa (S. Mahboob).
Peer review under responsibility of King Saud University.

Production and hosting by Elsevier

https://doi.org/10.1016/j.sjbs.2020.11.034
1319-562X/

produce fuels compatible with petrol and diesel (Banerjee et al., 2010). The expected second-generation fuels are biohydrogen, bio methanol, Fischer Troph diesel, biohydrogen, biodiesel and bioethanol (Alvira et al., 2009). The biochemical conversion methods are adopted to convert biomass into bioethanol. The third-generation biofuels are extracted from algae, which are referred to as "Oilgae". Researchers work on this new source, yielding biofuel ten times greater than conventional feedstock with less cost (Xu et al., 2009). The fourth-generation fuel research focuses on producing petrol from vegetable oil and biodiesel. Our focus is to produce ethanol from cellulose and hemicellulose and derives new technology to produce it from the bulk of plant matter rather than from starches and sugars (Carriquiry et al., 2011). Ethanol is used in flexible fuel vehicles with a higher blend of E85 that curtails CO emissions and has more octane rates. Biomass can supplement the use of petrochemicals (Keenan, 1981). Bioethanol produced by fermentation could resolve the energy crisis (Ward et al., 2006). Bioethanol production on a large scale by fermentation creates opportunities for new forms of energy (Akhir et al., 2009; Turhan et al., 2010). Bioethanol can be used as a transportation fuel to substitute petrol (Balat, 2011). Bioethanol can be produced from starches or celluloses that contain sugars (Sarkar et al., 2012). Bioethanol produced from food crops like sugarcane, wheat, and corn will impact food prices, slamming food security (Gon Wi et al., 2013; Mohanty et al., 2008; Douglas et al., 2012).

2. Material and methods

2.1. Substrate

The *Allamanda schottii* flowers were collected from VIT, Vellore campus, and the substrate's physiochemical characteristics were studied. The collected flowers were cleaned and stored in sealed polythene covers. The *Saccharomyces cerevisiae* strain was acquired from a domestic shop (as a dried yeast powered). Its physical and chemical properties characterized the withered flowers.

2.2. Inoculum preparation

The known weight of dried yeast pellets in sterilized YPD broth (yeast extract – 1%, peptone- 2%, dextrose – 2%, pH 4.5) was used for preparing the inoculum. The incubation period for culture media was 72–120 h under 37 °C. The serial dilution and plating techniques were used to assess the inoculum size and sterilized media was used to adjust the sample's cell concentration to 10^9/ml.

2.3. Screening of bioethanol production by yeast strains

Samples of different volumes were taken and inoculated with different inoculum sizes (1% and 2%). Incubation of samples was done at 37 °C for 5 days. After five days, pH changes in the sample and ethanol production were analyzed. This process was done in triplicates.

2.4. Fermentation

The *Allamanda* flower powder and distilled water are mixed in the ratio 10 g: 80 ml to form a slurry. An autoclave was used to mix the contents under 120 °C. The yeast strain *Saccharomyces cerevisiae* 3.0 g 100 ml^{-1} were prepared and added to the contents at 30 ± 2 °C. The slurry (1:6) was subjected to centrifugation under 200 rpm for about 15 min and allowed to ferment (Talebnia et al., 2011). The slurry pH was maintained at 5.5 to obtain the most acceptable results. This experiment was repeated 3 times (Johansson et al., 2014).

2.5. Distillation

The fermented broth was removed after 5 days to check for the presence of ethanol. The Whatman no.1 filter paper is used for collecting the supernatant from the fermenting slurry. The filtrate is heated after transferring it to a round bottom flask with a heating mantle (ILECO – 300 W- capacity 1000 ml). The separation ethanol occurred at 78.5 °C (boiling point of ethanol). Water was circulated to condense ethanol vapors from the condenser and collected in the distillate.

2.6. Immobilization

Immobilized microorganisms were utilized for fermentation. The support materials such as sodium alginate, jute fiber, bagasse and coconut coir were studied for bioethanol fermentation (Gokgoz and Yigitoglu, 2013). Fermentation media contains 10% glucose, 5 gm peptone, 5 g yeast extract, 1 g $MgSO_4$, and 1 gm K_2PO_4 in 1 L distilled water. Batch fermentation was conducted under 30–32 °C with an incubation period of 24 h incubation. During fermentation, the samples were analyzed for the depletion of polysaccharides and the amount of bioethanol synthesized.

2.6.1. Immobilization with sodium alginate

Sodium alginate (1% (w/v) solution was prepared and kept 24 h under agitation at 100 rpm. An aqueous solution of $CaCl_2$ (2%) was added drop by drop. The contents were agitated for 25 min. The solution was kept under vacuum at a 300 mm Hg pressure for 90 min to remove the gas. The solution was poured into a petri dish for drying at 50 °C in a hot air oven for 24 h after a day. The beads were immersed in a 2% calcium chloride solution (w/v) for 1 h and then dried for 48 h under 24 °C. Then the beads were stored in deionized H_2O for 3 days at 4 °C. These beads were then added to the fermentation medium. DNSA method was adopted to measure the concentrations of glucose and ethanol.

2.6.2. Immobilization with jute fiber

The jute's molecular and structural parameters can open up new avenues for its proper utilization Jute fiber procured locally, were thoroughly washed and dried. It was cut into 50 mm pieces and sterilized. The concentrated cell suspension was sprayed over jute fiber aseptically and left for 3 h (Xie and Ma, 2009).

2.6.3. Immobilization with sugarcane bagasse

Bagasse, procured locally, was thoroughly washed, dried and pith chopped into 50 mm pieces for cell loading. The sugarcane bagasse was subjected to dry in air and maintained under room temperature. In a 500 ml Erlenmeyer flask 2.5 g of sterile sugarcane bagasse was mixed with 50 ml of yeast suspension and allowed to incubate under *30–32 °C* in a shaker at 100 rpm for 24 h. This procedure is termed immobilization. After the incubation period, 100 ml of sterile distilled H_2O was added to wash the decanted sample.

2.6.4. Immobilization with coconut coir

Coconut coir is a significant underused raw material that contains more cellulose, nearly 32– 43% of its dry weight (Ayrilmis et al., 2011). Reports prove that the coconut fibers are being used in the polymer composite field (Geethamma et al., 1995). The coconut coir has main components such as cellulose, lignin and hemicellulose. The cellulose has crystalline nature, whereas the lignin is amorphous. CCF samples were obtained from a local market

and the impurities were removed after rinsing it with water and then dried (48 °C) for 48 hrs. Cell loading was done on coconut coir.

2.7. Preparation of magnetic nanoparticles

The co-precipitation technique with slight modification was applied for preparing the nanoparticles (Xie and Ma, 2009). A round bottom flask $FeSO_4{\cdot}7H_2O$ (2.78 g) was mixed with FeCl3·.6H2O (5.4 g) by dissolving 100 ml of deionized water at a molar ratio 1:2. The contents were mixed using a magnetic stirrer continuously at 80 °C. One sodium hydroxide mole was added drop by drop continuously to reach pH 10, which resulted in a black precipitate formation. Then was washed 4–5 times in deionized H_2O and dried at 60 °C overnight and stored to further. FTIR, SEM, and XRD analysis were used for the characterization of the synthesized catalyst

2.7.1. Immobilization of cellulase to magnetic nanoparticles

Covalent binding Cellulase enzyme (5 mg/mL) with the nanoparticle was done by incubating it for 120 min under 25 °C mixed in a shaker at 250 rpm. The nanoparticle's immobilized enzyme was cleaned with deionized H_2O and buffered to remove weakly bound cellulose (Gokhale et al., 2013). Morphological analysis with and without immobilization was studied using SEM, FTIR and XRD.

2.7.2. Immobilization efficiency

To calculate the immobilization efficiency was calculated by measuring the activity of cellulose enzyme present in the pre and post immobilized solution with the following formula:

$$\text{Rate of immobilization efficiency} = [(\text{EoVo-EfVf})/\text{EoVo}] \times 100$$

Where

Eo is the initial cellulase activity (U/ml)

Vo, the initial volume of cellulase solution (ml) Ef the cellulase activity of the filtrate (U/ml) Vf, is the filtrate volume (ml)

2.8. Fabrication of bioethanol production by SSF

In solid-state fermentation (SSF) the complex lignocellulose materials are broken to form simple sugars by cellulose enzyme action and fermentation producing bioethanol. The yeast *Saccharomyces cerevisiae* is commonly used to produce bioethanol because it has maximum efficiency in sugars to bioethanol (Johansson et al., 2014). A 250 ml flask was used for mixing 1 g of floral powder in 100 ml citrate buffer followed by the addition of yeast extract and 0.1% - peptone and after sterilization, this media was subjected for inoculation with 5 ml of free or immobilized enzyme. The fermentation process occurred under 30 °C at 100 rpm. At regular 10 h of the interval, the samples were analyzed for residual sugar and ethanol concentration.

2.9. Immobilized cellulase enzyme activity assay

The reducing polysaccharides were found out by the DNSA method (Strehaiano et al., 2006). About 1% CMC was dissolved in 50 mmols/Litre of sodium acetate (pH 4.8). This mixture was kept in incubation for 15 min at 50 ± 2 °C. 3 ml of DNS reagent (3 ml) after its addition to the above mixture and kept in incubation under *100 °C* for 10 min. 1.5 ml Rochelle salt was added to the incubated DNS reagent and then it was cooled. The optical density was measured at 620 nm. The amount of enzyme that releases one μmol of reducing sugars in one minute is referred to as IU (one unit of cellulase activity).

2.10. Cellulase enzyme stability on various parameters

2.10.1. Study of thermal stability

The influence of temperature on cellulase activity was determined under both free and immobilized condition. The substrate was incubated at a temperature range of 40 °C –90 °C for 1 hr with free enzymes and immobilized enzymes (Van Uden, 1984).

2.10.2. Study of pH stability

The cellulase stability in the free and immobilized state was noticed when pH was maintained in a range of 1.0 to 5.0 for 1 h, both free and immobilized enzymes on the buffer solution.

2.10.3. Recycling of immobilized cellulase

The reusability of the immobilized cellulase was noted by using it several times for the hydrolysis. Phosphate buffer (pH 7.0) was used for storing free and immobilized cellulose at 5 °C for 60 days to study its storage stability. With 10 days interval, the enzymatic activity was studied using the titration method and formula 7.1 was used for calculation.

2.10.4. Ethanol blending and emissions

The Single cylinder 4 Stroke Petrol engine (Fig. 1) operating with a blend of petrol and bioethanol of 0%, 5%, 10%, 15% and 20% were tested under different engine speeds. Fuel consumption was measured using measuring glass. The basic engine parameters such as torque, power and specific fuel consumption were studied at engine speeds of 1600–3400 rpm. The blend of 95% petrol and 5% bioethanol and petrol were tested in a single-cylinder four-stroke petrol engine test rig with an electric brake dynamometer. The gas analyzer QROTECH (model QRO-402) – 4 gas Analyzer was used for engine diagnosis. The gas analyzer reveals the exhaust gas level from the engine fueled by bioethanol doped petrol.

3. Results

3.1. Characterization of flower

The withered flowers have been characterized for moisture content, total solids, ash content and total sugars, which was listed in Table 1.

3.2. Screening on the substrate for the presence of ethanol

The screening results also show that the ethanol concentration for slurry volume 1:1 decreases on the 5th day of incubation, whereas the slurry volume 2:1, there is no change in ethanol production. The screening gives the idea that the substrate selected can be further studied for the production of ethanol. The shade dried flowers were taken for analysis. The supernatant collected after fermentation was distilled to get ethanol. Ethanol without moisture was acquired by keeping the distillate in the refrigerator to maintain the freezing temperature. The H_2O molecules existing in the sample freezes at 0 °C and 99.50% clean ethanol (freezing point −117 °C) was obtained and stored. 10 ml of bioethanol for 100 ml of the slurry was obtained.

3.3. Confirmation for the presence of ethanol

LC-MS is a technique to combine liquid chromatography (HPLC) and mass spectrometry (MS). LC separates the components based on their liking of a sample with a liquid or solid phase and detecting the separated components using ultraviolet or electrical conductivity based on their properties. Detection is done based on intensity and area on high peaks with retention time. Mass

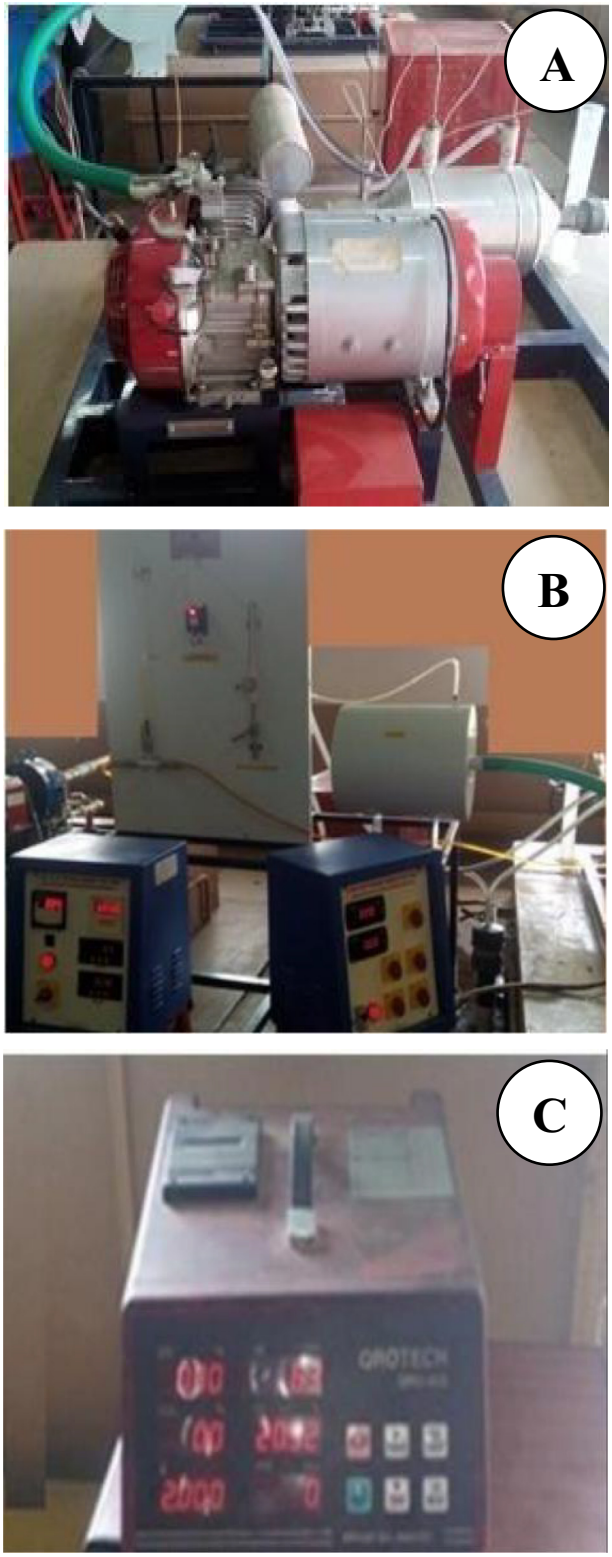

Fig. 1. Engine testing of produced bio-ethanol A) Single cylinder 4 S petrol engine; B) Single cylinder four stroke engine test rig; C) Four gas analyzer.

spectrometry is a susceptible technique where the samples are detected. The presence of ethanol was confirmed with the use of LCMS. The LC confirmed by LC results confirmed the existence of bioethanol in sample distillates. (Fig. 2). Dimethyl ether, Propanol, Iso-butane, Methyl nitrate, Hexane, Acetaldoxime, Malononitrile were the other component present in low quantities with the ethanol distillate revealed by the MS report

Table 1
Characterization of flower waste.

Parameters	Value
Moisture content (wet basis)	79.40%
pH	6.5
Total solids	22%
Ash content	2.40%
Total sugars	60–65%

3.4. Crystallinity index

3.4.1. Analysis of crystallinity index of sodium alginate

The XRD peaks obtained were compared with the standard reference Joint Committee of Powder Diffraction Standards (JCPDS) file for sodium alginate. The peaks show hemicellulose and lignin in the substrate, which could be removed by pretreating the substrate. The peak Indexed No is 80–0020 with 6 major diffraction peaks as a result of reflections from the (111), (200), (220), (311), (222), (420) and (422) planes.

3.4.2. Analysis of crystallinity index of jute fiber

The most crucial approach in the estimation of crystalline cellulose is x-ray diffraction. It gives the proportions of amorphous and crystalline components present. The application of this method to jute indicates the presence of crystalline cellulose present in jute. The vital chemical group present in jute fiber are the hydroxyl (–OH) group and the methyl group (CH_2OH). Because of these groups, the hydrogen bonds dominate between OH group and jute fiber compared to van der Waals forces. The OH groups in amorphous regions are more reactive than those in the crystalline region. The jute fiber revealed the 2θ peaks at 22.50 and 16.40 due to lignin and hemicelluloses, respectively.

3.4.3. Analysis of crystallinity index of sugarcane bagasse

The X-ray diffraction study for bagasse indicates the peak at 2θ = 15.5 and 20.5 indicates amorphous hemicellulose by sweeping curves and crystalline cellulose by peaks. XRD of the sugarcane bagasse shows the crystalline and amorphous phases obtained and compared with the data from ICDD.

3.4.4. Analysis of crystallinity index of coconut coir

The diffraction shows narrow peaks indicating the crystalline part of the material, while the broader peaks show the amorphous part of fibers. It gives us the idea that the diffraction patterns of the coir have low crystallinity (amorphous). The amorphous characteristic of coconut coir is due to the high lignin content. Generally, lower crystallinity in lignocellulosic materials is due to the presence of more lignin and hemicellulose. The Bragg angles at 16°, 22° and 35° show cellulose characteristics and the peak at Bragg angle 2θ of 22°corresponds to the crystalline region.

3.5. Growth studies

Growth studies of *Saccharomyces cerevisiae* using free and immobilized cells in jute fiber, bagasse, coconut coir and sodium alginate were studied. The batch fermentation at 32 °C was carried out using free *Saccharomyces cerevisiae cells* and immobilized *Saccharomyces cerevisiae* cells on to substrates such as sodium alginate, jute fiber, sugarcane bagasse, and coconut coir, respectively. From Fig. 3 it was seen that the growth rate of free cells was more than that of immobilized cells. The growth rates were seen as calcium alginate (12.2 g/L), jute fiber (10.50 g/L), bagasse (10.00 g/L) and coconut coir (9.0 g/L) at 12 h. The lower growth rate was seen in immobilized cells than free cells (16.4 g/L) due to space shortage for growth and mass transfer limitation of nutrients.

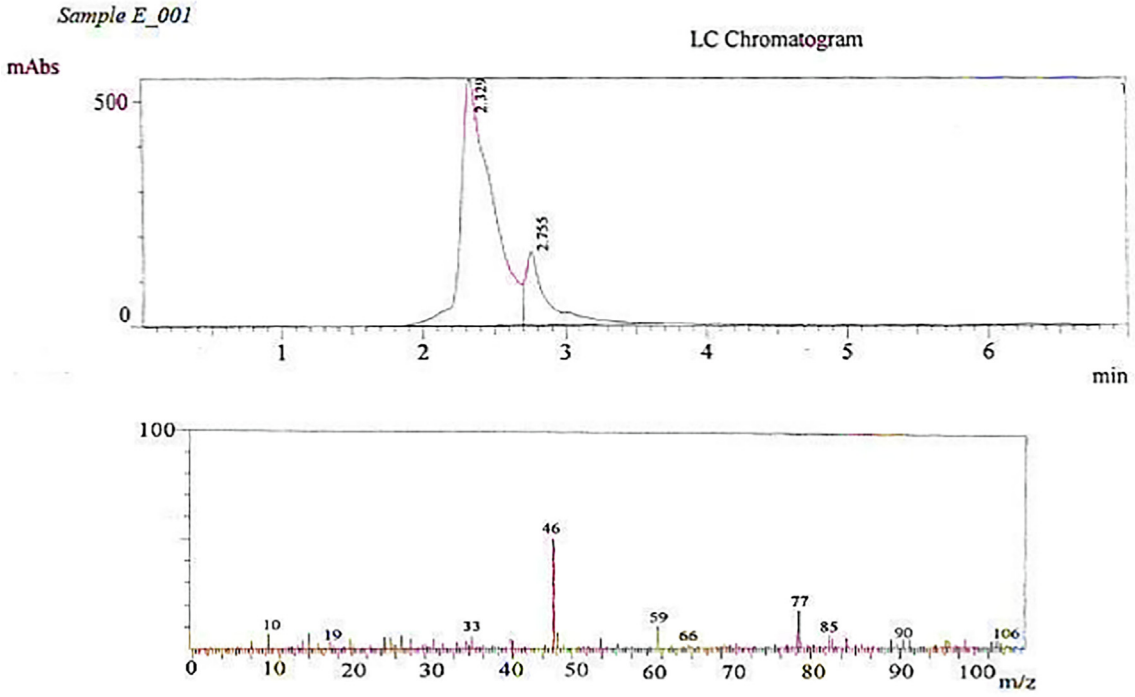

Fig. 2. LCMS report shows the presence of ethanol.

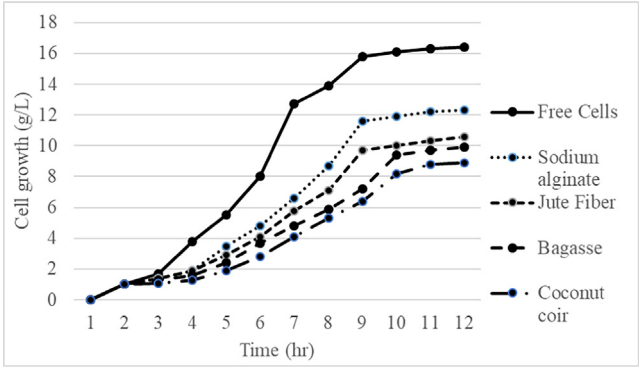

Fig. 3. Cell growth on different substrates.

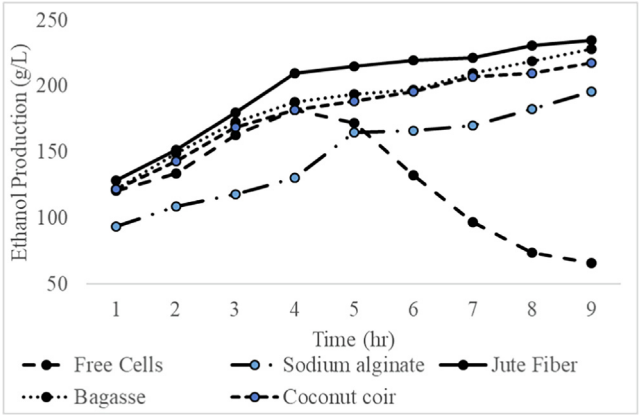

Fig. 4. Ethanol production on different substrates.

3.6. Ethanol production

The inward dispersal of nutrients and outward dispersal of ethanol is slowed down due to the substrates' physical barriers. From Fig. 4, the ethanol production was found to be maximum in jute fiber (235 g/L) followed by sugarcane bagasse (228 g/L), coconut coir (218 g/L), and sodium alginate (196 g/L) as compared to free cells(182 g/L).

3.7. Magnetic nanoparticle characterization

The co-precipitation technique was adopted for synthesizing the magnetic nanoparticle using FeSO4.7H2O and FeCl3.6H2O (Raita et al., 2015). To test the magnetic property of nanoparticle, a magnet was brought near to the particles and it was seen that the nanoparticles flocks towards the magnet showing the presence of ferrous constituent. To study the external structure of the synthesized magnetic nanoparticle, SEM was used. Ferro nanoparticle's surface were analyzed by scanning electron microscopy with an electron beam at 5 kV energy (Figure not shown). The presence of any impurities other than Fe and O in the magnetic nanoparticle was analyzed using advanced SEM-EDAX. Also, Table. 2 gives the calculated by EDAX.

The FT-IR spectrum of the magnetic nanoparticle was studied. The characteristic absorption peak at 551.64 cm-1 shows Fe-O stretching vibrations of Fe_3O4. A peak shows that a hydroxyl group was present in the synthesized magnetic nanoparticle at 3134.33 cm^{-1}. The FTIR spectra confirmed the formation of magnetic nanoparticles. The results acquired from FTIR correlates with the previously reported FTIR spectrum for magnetic nanoparticles (Stambuk et al., 2009). The crystallinity of synthesized Fe3O4 mag-

Table 2
EDAX value for the synthesized nanoparticle.

	Weight %	Atomic %
O	30.70	60.73
Fe	69.30	39.27

netic nanoparticles was studied using X-ray diffraction. The XRD pattern on Fe_3O_4 magnetic nanoparticles reveals that the diffraction peaks at 220, 311, 400, 422, 511 and 440 are the characteristic peaks of the Fe_3O_4 crystal with cube structure. The diffraction peaks are compared with those given in the JCPDS index (no.65–3107). The average crystalline size of the sample was estimated at 20 nm.

3.8. Characterization of immobilized cellulase

The APTES through EDC and NHS facilitated the successful immobilization of cellulase enzyme to the surface's synthesized magnetic nanoparticles. After the cellulase enzyme's immobilization, the surface of magnetic nanoparticles was rough due to the formation of protein layers along with nano-pores (Fig. 5).

3.9. Evaluating the rate of immobilization

The degree of cellulase immobilization with the MNPs was found to be 86%. The establishment of a covalent bond between the amino functional group of the cellulase and aldehyde group present in the MNPs surface resulted in immobilizing the enzyme to MNPs.

3.10. Stability of cellulase enzyme under different parameters

3.10.1. The temperature on enzyme activity

The optimal temperature for both free cellulase and immobilized cellulase enzymes were analyzed between 40 °C and 80 °C. (Fig. 6A). It was found that the activity of free enzyme showed a maximum at 60 °C and it began to drop when the temperature increased (Beltrn et al., 2007; Torija et al., 2003). The cellulase activity was shallow at temperature 80 °C because of activity loss. The enzymatic activity of cellulase immobilized magnetic nanoparticle was stable even under 80 °C, but maximum activity was noticed at 60 °C.

3.10.2. pH on enzyme activity

The pH level on free enzyme and immobilized cellulase enzyme was studied under a pH of 4.0–8.0 (Akrida-Demertzi et al., 1988). Fig. 6B shows that the change in pH changed in cellulose activity of the free and immobilized enzyme. The immobilized biocatalyst cellulase activity was maximum at pH 6, whereas the cellulose activity for free enzymes showed a lesser pH of 5.

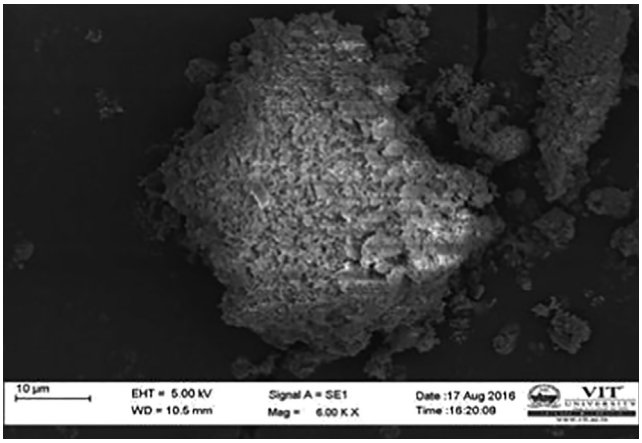

Fig. 5. SEM Image of cellulase on magnetic nanoparticle.

3.10.3. Stability of immobilized cellulase

Fig. 6C shows the stability of free and immobilized cellulase enzyme with the substrate. The stability of the immobilized cellulase was higher when compared with the free enzyme. The Immobilized cellulose enzyme on Fe3O4 nanoparticles showed a gradual decrease after every 1-hour interval. The immobilized enzyme was capable of having 95% of its originality after 2 h. The immobilized enzyme retained 80% originality after 5 h of reaction time. The stability of free enzymes decreased sharply. This indicates that immobilized cellulose enzyme stability on Fe_3O_4 nanoparticles gets inactivated at slower rates than free enzymes. The immobilized enzyme's storage stability exhibited a value more than the free cellulase enzyme as its activity remained unchanged for nearly 1440 h.

3.10.4. Reusability of immobilized cellulase

In large scale and commercial applications, the repeated use of biocatalyst will curtail an enzyme's price. The repeated use of immobilized enzymes was carried out for hydrolyzing the cellulose. For every single use, the nanoparticles are separated by using a magnet and washed with deionized water. Fig. 6D shows the reusability of immobilized enzymes and this gives us an understanding of its activity. The immobilized enzyme was repeatedly used for 5 cycles. It was seen that the originality maintained by the enzyme was 60%.

3.11. Bioethanol production by SSF

The lignocellulosic biomass consists of lignin 20–30%, hemicellulose 20–40% and cellulose 40–50%. In this study, the horticultural waste material *Allamanda* flowers were used to produce bioethanol. The flower powder was pre-treated with 0.5 mol/L NaOH and sterilized after the addition of peptone and yeast. Then this media was inoculated with an immobilized enzyme in one flask and free enzymes with another flask. Fig. 6E and 6F show that the immobilized enzymes produce more reducing sugars (25 g/ml) than free enzymes (18 g/ml). The highest ethanol production using SSF was about 182 g/L and 252 g/L, respectively, with free and immobilized cellulase enzymes.

3.12. Performance and emission analysis

3.12.1. Engine torque

The ability to produce useful work in an engine is termed as torque**.** The engine torque rises with engine speed and after reaching maximum torque, it reduces with an increase in engine speed. The Fig. 7A shows the influence of bioethanol and petrol blend fuels on torque output. The highest output torque of 10.75 Nm occurred at an engine speed of 3200 rpm for the E20 blend. This was due to higher air mixing with the fuel to increase the torque.

3.12.2. Brake power

The brake power is directly proportional to torque output. The breaking load was by electric brake dynamometer; with the increase in braking load and engine speed, the engine torque increases. The increase in bioethanol content in the blend will increase the power output of the engine. Fig. 7B clearly shows a higher value of brake power as 4 kW at an engine speed of 3400 rpm for the E20 blend.

3.12.3. Specific fuel consumption

Fig. 7C relates the engine speed with SFC for different blends of bioethanol and petrol. The SFC shows a decreased value with the increase in bioethanol content in the blend. At 3400 rpm of engine

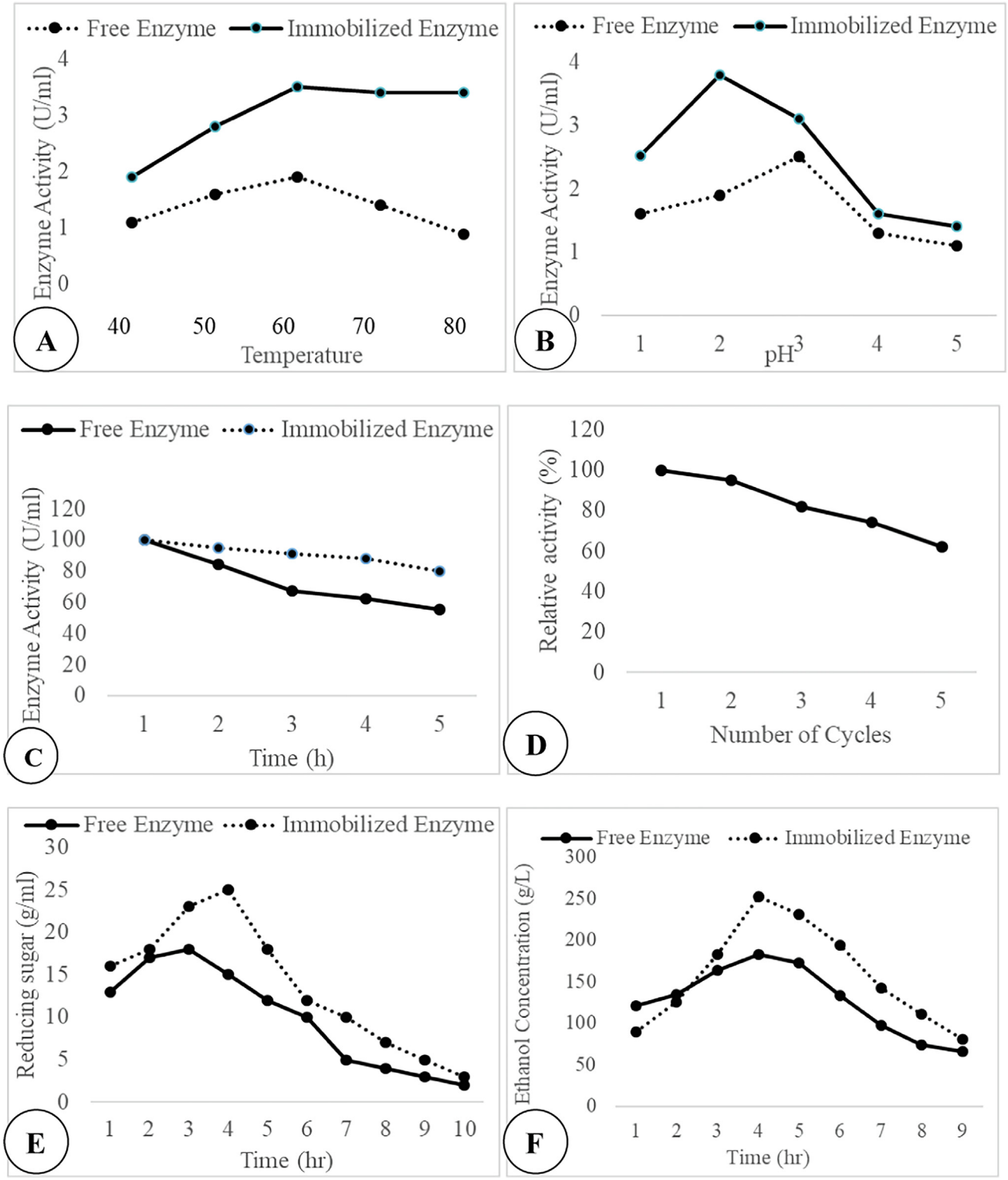

Fig. 6. Enzyme characterization; (A) Temperature on enzyme activity; (B) pH on enzyme activity; (C) Stability of free and immobilized enzyme; (D) Reusability of immobilized enzyme; (E) Reducing sugar concentration in fermentation (F) Ethanol concentration in SSF.

speed, combustion fuel showed a lower value for the blend E 20 as 267g/kWh. This is because the calorific value of bioethanol is less compared to petrol. To produce the same power as petrol, bioethanol should be 1.5 times greater than petrol. The specific fuel consumption was 308g/kWh at 3400 rpm of engine speed while using petrol.

3.13. Emission studies

3.13.1. Carbon monoxide emissions

CO is an indicator that shows richness in the air–fuel mixture. Bioethanol has 35% oxygen content. The more oxygen content will ensure better mixing of O2 to fuel ratio, which leads to good com-

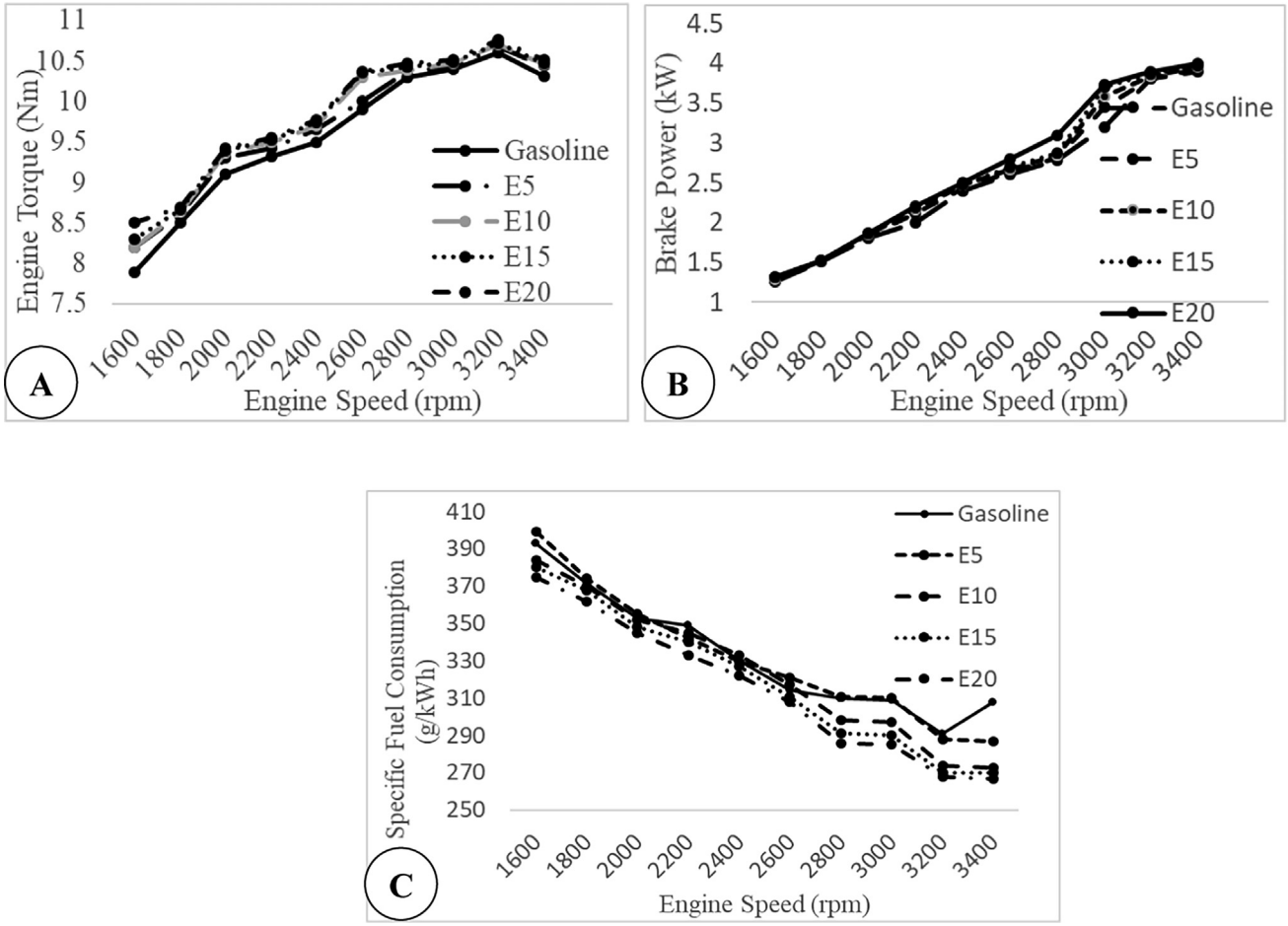

Fig. 7. Performance characterization of Bio-ethanol. (A) Engine Torque Studies with Various Blends of Bioethanol and Petrol; (B) Engine Brake Power Studies with Various Blends of Bioethanol and Petrol (C) Engine SFC Studies with Various Blends of Bioethanol and Petrol.

bustion. As a result, more carbon molecules are burnt, resulting in complete combustion by releasing CO_2. Because of complete combustion, the release of CO was nil. For an adequately run engine, the CO emission is between 0.5% and 1%. Fig. 8A shows a high CO value as 6.82%, which indicates the engine is running rich.

3.13.2. Hydrocarbon emissions

HC emission indicates the fuel, whether rich or lean, causing a misfire. Any HC in the exhaust gas is unburned fuel. Engine out HC emission may be as high as 500 ppm at idle. Fig. 8B shows the maximum HC as 231 ppm and within permissible limits.

3.13.3. Carbon dioxide emissions

CO_2 has indicated the efficiency of combustion. More O2 or less O2 levels than the stoichiometric air–fuel ratio indicates the mixture is lean or rich. When the engine runs at stoic CO_2 is about 12 – 15%. Fig. 8C shows that CO_2 is below 12%.

3.13.4. NOX emissions

NOX is a chemical bonding of nitrogen and oxygen. NOX is the most difficult of the three regulated emissions to convert. A normal NOX reading should be no more than 100 ppm at idle and not more than 1000 ppm at a steady load. The Fig. 8D shows the NOX level as 802 ppm for engine speed 2941 rpm, under the permissible limit.

4. Discussion

Ethanol synthesis from the microbe was screened and usually the production of by-products such as lactate, acetate, glycerol and acetone will eventually decrease the ethanol production (Najafpour et al., 2002), Jute fiber was more suitable for more ethanol production because jute fiber has more porosity and has better assimilative capabilities than other substrates (Bafrncovo et al., 1999). Ethanol production showed a distinct peak, increasing up to a certain level and then decreasing gradually in free cells. It would have occurred due to cell leakage. This leakage reduces cells available for production and there is a declining trend seen in ethanol production. A cell to carrier ratio (9:1) is optimum for maximum production of ethanol (D'Amore et al., 1989). The structure shown was clear and smooth (Raita et al., 2015). Aggregates ensured immobilization on the nanoparticle's surface and pair with the result obtained by Raita et al. (2015). The nano-sized pores were formed due to cellulase enzymes' surface binding with the MNPs (Huang et al., 2011). The immobilized biocatalyst cellulase activity becomes stable when the temperature elevated from 70 to 80 °C and this because the biocatalyst was denatured under elevated temperature (Talasila et al., 2011). The optimum temperature range may lead to the higher activation energy for the molecules to bind with the substrate and this activity of the enzyme to function well is the main advantage of enzyme immobilization (Wijeyaratne, 1998). The pH plays a vital role in enzyme activity. It depends on its functional groups. Immobilizing enzymes with a substrate can also shift its activity's pH range (Zertuche and

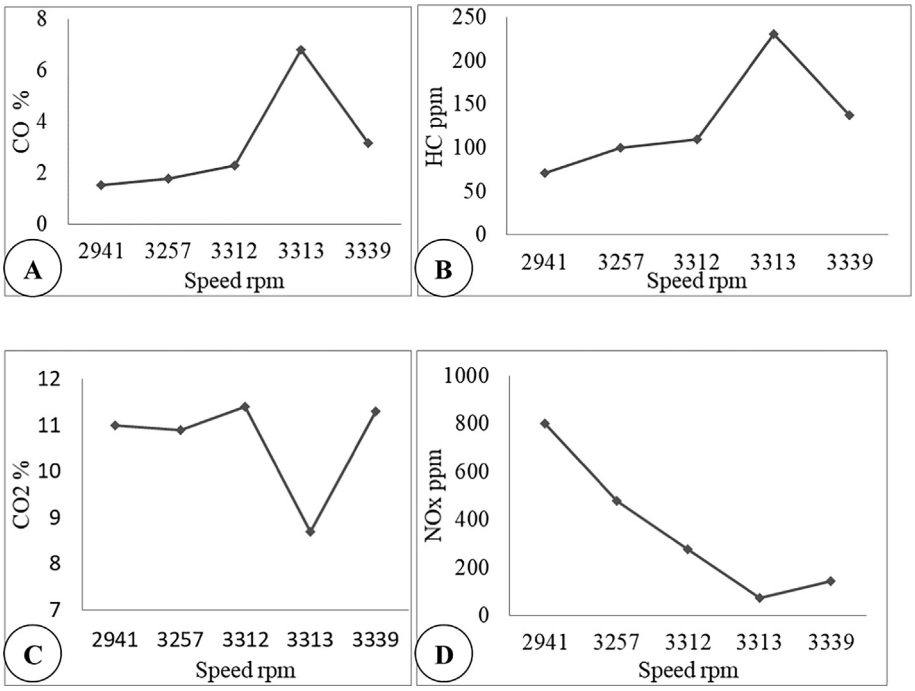

Fig. 8. Emission Characteristics of Bio-ethanol. (A) Emission of CO for Petrol –Bioethanol Blend at Various Engine Speeds (B) Emission of HC for Petrol –Bioethanol Blend at Various Engine Speeds (C) Emission of CO_2 for Petrol –Bioethanol Blend at Various Engine Speeds (D) Emission of NOX for Petrol –Bioethanol Blend at Various Engine Speeds.

Zall, 1985). The change in pH gives us information about the structure–function relationships of an enzyme. This increase in pH for the immobilized enzymes may be due to a rise in the net charge of magnetic nanoparticles binding with the enzyme (Akrida-Demertzi et al., 1988).

The stability of free enzymes decreased sharply (Liu and Shen, 2008; Al-judaibi, 2011). This indicates that immobilized cellulose enzyme stability on Fe_3O_4 nanoparticles gets inactivated at slower rates than free enzymes. The immobilized enzyme's storage stability exhibited a value more than the free cellulase enzyme as its activity remained unchanged for nearly 1440 h. This results in the values reported by Gokgoz and Yigitoglu (2013) on storage stability. Four cycles of cellulose enzyme use on Magneto responsive graphene showed 55% (Johansson et al., 2014). Immobilizations of cellulase with the magnetic nanoparticle boosted the enzymatic activity and enhanced the bioethanol production (Wu et al., 2010). The bioethanol added with petrol produces a lean mixture that increases the air–fuel ratio and makes combustion more efficient (Emiroğlu and Şen, 2018a). The addition of bioethanol in the blend will increase the output power (Hsieh et al., 2002). While using petrol, the specific fuel consumption was 308 g/kWh at 3400 rpm of engine speed (Kannan et al., 2012). The inadequate supply of oxygen for combustion shows high CO levels (Kwanchareon et al., 2007). the maximum HC as 231 ppm and within permissible limits (Shi et al., 2006). When the engine runs at stoic CO_2 is about 12 – 15%. Fig. 8C shows that CO_2 is below 12% (Yasar et al., 2015). shows the NOX level as 802 ppm for engine speed 2941 rpm, under the permissible limit (Zaharin et al., 2017).

5. Conclusion

The ethanol fermentation by using an immobilized cell was performed better than the free cell system. Immobilization techniques can improve cell concentration and thereby increases the production of ethanol. Since stability was better than the free cell system, this can be an attractive system to get more ethanol yield. The ethanol yield by immobilized Saccharomyces cerevisiae cells on jute fiber showed more than free cells and other substrates. Cellulase enzyme immobilized with a magnetic nanoparticle was very effective in improving enzyme activity to give more ethanol.

Acknowledgments

The authors extend their appreciation to the Deputyship for Research and Innovation, "Ministry of Education" in Saudi Arabia for funding this research work through the Project no. (IFKSURP-RGP-1435-012).

References

Abdel Ghany, T.M., Elhussieny, N.I., Rhaman, A., Shater, M.A., 2014. Biobeneficial spectrum of halophyte Plant *Avicennia marina* as a second generation of bioethanol production. J. Biol. Chem. Res. 31, 869–881.

Akhir, S.M., Abd-Aziz, S., Salleh, M.M., Rahman, R.A., Illias, R.M., 2009. Medium optimisation of chitinase enzyme production from shrimp waste using *Bacillus licheniformis* TH-1 by response surface methods. Biotechnol. 8, 120–125.

Akrida-Demertzi, K., Demertzis, P.G., Koutinas, A.A., 1988. pH and trace-elements content in raisin extract industrial-scale alcoholic fermentation. Biotechnol. Bioengg. 31, 666–669.

Al-judaibi, A.A., 2011. Effect of Some Fermentation Parameters on Ethanol Production from Beet Molasses by *Saccharomyces cerevisiae* CAIM13. Amer. J. Agricul. Biol. Sci. 6, 301–306.

Alvira, P., Pejo, E.T., Ballesteros, M., Negro, M.J., 2009. Pretreatment technologies for an efficient bioethanol production process based on enzymatic hydrolysis: A review. Bioresour. Technol. 101, 4851–4861.

Ayrilmis, N., Jarusombuti, S., Fuengvivat, V., Bauchongkol, P., 2011. Effect of thermal treatment of rubber wood fibres on physical and mechanical properties of medium density fibreboard. J. Trop. For. Sci. 23, 10–16.

Bafrncovo, P., Smogrovicova, D., Slavikova, I., Patkova, J., Domeny, Z., 1999. Improvement of very high gravity ethanol fermentation by media supplementation using *Saccharomyces cerevisiae*. BiotechnoL. Letters. 21, 337–341.

Balat, M., 2011. Production of bioethanol from lignocellulosic materials via the biochemical pathway: A review. Ener. Convers. Manage. 52, 858–875.

Banerjee, S., Mudliar, S., Sen, R., Giri, B.S., 2010. Commercializing lignocellulosic bioethanol: Technology bottlenecks and possible remedies. Biofuel. Bioprod. Biorefining. 4 (1), 77–93.

Beltrn, G., Rozas, N., Mas, A., Guillamom, J., 2007. Effect of low temperature fermentation on yeast nitrogen metabolism. World. J. Microbiol. Biotechnol. 23, 809–815.
Carriquiry, M.A., Du, X., Timilsina, G.R., 2011. Second generation biofuels: Economics and policies. Energy. Policy. 39, 4222–4234.
D'Amore, T., Celotto, G., Russell, I., Stewart, G.G., 1989. Selection and optimization of yeast suitable for ethanol production at 40°C. Enzyme. Microbial. Technol. 11, 411–416.
Douglas, J.B., Bowman, M.J., Braker, J.D., Dien, B., Hector, R.E., Lee, C.C., Mertens, J.A., Wagschal, K., 2012. Plant Cell Walls to Ethanol. Biochem. J. 442, 241–252.
Emiroğlu, A.O., Şen, M., 2018. Combustion, performance and emission characteristics of various alcohol blends in a single cylinder diesel engine. Fuel 212, 34–40.
Geethamma, V.G., Joseph, R., Thomas, S., 1995. Short coir fiber-reinforced natural rubber composites: effects of fiber length, orientation and alkali treatment. J. Appl. Polym. Sci. 55, 583–594.
Gokgoz, M., Yigitoglu, M., 2013. High productivity bioethanol fermentation by immobilized *Saccharomyces bayanus* onto carboxy methyl cellulose-g- poly (N-vinyl-2-pyrrolidone) beads, Artificial Cells. Nanomed. Biotechnol. 41, 137–143.
Gokhale, A.A., Lu, J., Lee, I., 2013. Immobilization of cellulose on magneto responsive graphene nano-supports. J. Mol. Catal B. Enzym. 90, 76–86.
Gon Wi, S., Choi, I.S., Kim, K.H., Kim, H.M., Jong, H., 2013. Bioethanol production from rice straw by popping pretreatment. Biotechnol. Biofuels. 6, 166.
Hsieh, W.D., Chen, R.H., Wu, T.L., Lin, T.H., 2002. Engine performance and pollutant emission of an SI engine using ethanol–gasoline blended fuels. Atmos. Environ. 36, 403–410.
Huang, X.J., Chen, P.C., Huang, F., Ou, Y., Chen, M.R., Xu, Z.K., 2011. Immobilization of Candida rugosa lipase on electrospun cellulose nanofiber membrane. J. Mol. Catal. B Enzym. 70, 95–100.
Johansson, E., Xiros, C., Larsson, C., 2014. Fermentation performance and physiology of two strains of *Saccharomyces cerevisiae* during growth in high gravity spruce hydrolysate and spent sulphite liquor. BMC. Biotechnol. 14, 47.
Kannan, D., Pachamuthu, S., Nabi, M.N., Hustad, J.E., Løvås, T., 2012. Theoretical and experimental investigation of diesel engine performance, combustion and emissions analysis fuelled with the blends of ethanol, diesel and Jatropha methyl ester. Ener. Convers. Manag. 53, 322–331.
Keenan, M.H.J., 1981. Solute transport and plasma-membrane lipid composition in *Saccharomyces cerevisiae* NCYC 366 Ph.D. thesis. University of Bath, pp. 115–117.
Kongkiattikajorn, J., Sornvoraweat, B., 2011. Comparative Study of Bioethanol Production from Cassava Peels by Monoculture and Co-Culture of Yeast, Kasetsart. J. Nat. Sci. 45, 268–274.
Kwanchareon, P., Luengnaruemitchai, A., Jai-In, S., 2007. Solubility of a diesel–biodiesel–ethanol blend, its fuel properties, and its emission characteristics from diesel engine. Fuel 86, 1053–1061.
Liu, H., Sun, J., Chang, J.S., Shukla, P., 2018. Engineering microbes for direct fermentation of cellulose to bioethanol. Criti. Rev. Biotechnol. 38, 1089–1105.
Liu, R., Shen, F., 2008. Impacts of main factors on bioethanol fermentation from stalk juice of sweet sorghum by immobilized *Saccharomyces cerevisiae* (CICC 1308). Bioresour. Technol. 99, 847–854.
Mittal, G.S., 1992. Food Biotechnology: Techniques and Applications. Technomic Publishing Co., New York, Lancaster.
Mohanty, S.K., Behera, S., Swain, M.R., Ray, R.C., 2008. Bioethanol production from Mahula (*Madhuca latifolia* L.) flowers by solid-state fermentation. Appl. Ener. 86, 640–644.
Najafpour G.D., Zizan A.A. and HarunKamaruddin A., 2002. Microbial desulfurization of malaysian coal in batch process using mixed culture, Int. J. Eng.,15(3), 227-234.
Raita, M., Arnthong, J., Champreda, V., Laosiripojana, N., 2015. Modification of magnetic nanoparticle lipase designs for biodiesel production from palm oil. Fuel Process. Technol. 134, 189–197.
Raita, M., Ibenegbu, C., Champreda, V., Leak, D.J., 2016. Production of ethanol by thermophilic oligosaccharide utilising *Geobacillus thermos glucosidasius* TM242 using palm kernel cake as a renewable feedstock. Biomass. Bioener. 95, 45–54.
Rankovic, J., Dodic, J., Dodic, S., Popov, S., 2009. Bioethanol Production From Intermediate Products of Sugar Beet Processing With Different Types of Saccharomyces cerevisiae. Chem. Ind. Chemical. Engg. Qua. 15, 13–16.
Sarkar, N., Ghosh, S.K., Bannerjee, S., Aikat, K., 2012. Bioethanol Production from Agricultural Wastes: An Overview. Renewable Energy 37, 19–27.
Shi, X., Pang, X., Mu, Y., He, H., Shuai, S., Wang, J., Chen, H., Li, R., 2006. Emission reduction potential of using ethanol–biodiesel–diesel fuel blend on a heavy-duty diesel engine. Atmos. Environ. 40, 2567–2574.
Stambuk, B.U., Dunn, B., Alves Junior, S.L., Duval, E.H., Sherlock, G., 2009. Industrial fuel ethanol yeasts contain adaptive copy number changes in genes involved in vitamin B1 and B6biosynthesis. Genome Res. 19, 2271–2278.
Strehaiano, P., Ramon-Portugal, F., Taillandier, P., 2006. Yeasts as biocatalysts, Yeasts in Food and Beverages, pp. 243–283, Springer, 2006.
Talasila, U., Vechalapu, R.R., Beebi, S.K., 2011. Optimization of fermentation conditions for the production of ethanol from cashew apple juice using doehlert experimental design. J. Microb. Biochem. Technol. 3, 004–008. https://doi.org/10.4172/1948-5948.1000042.
Talebnia, U., Vechalapu, R.R., Shaik, K.B., 2011. Optimization of Fermentation Conditions for the Production of ethanol From Cashew Apple Juice using Doehlert Experimental Design. J. Microb. Biochem. Technol. 03, 2011.
Talebnia, F., Karakashev, D., Angelidaki, I., 2010. Production of Bioethanol from Wheat Straw: An Overview on Pretreatment, Hydrolysis and Fermentation. Bioresour. Technol. 101, 4744–4753.
Torija, M.J., Rozes, N., Poblet, M., Guillamón, J.M., Mas, A., 2003. Effects of fermentation temperature on the strain population of *Saccharomyces cerevisiae*. Int. J. Food. Microbiol. 80, 47–53.
Turhan, I., Bialka, K.L., Demirci, A., Karhan, M., 2010. Ethanol production from carob extract by using *Saccharomyces cerevisiae*. Bioresour. Technol. 101, 5290–5296.
Van Uden, N., 1984. Temperature profiles of yeast. Adv. Microb. Physiol. 25, 195–248.
Ward, O.P., Singh, A., Ray, R.C., 2006. Production of renewable energy from agricultural and horticultural substrates and wastes. In: Ray, R.C., Ward, O.P. (Eds.), Microbial biotechnology in horticulture, 1. Science Publishers, Enfield New Hampshire, pp. 517–558.
Wijeyaratne, S.C., 1998. Temperature tolerance and other properties of two ethanol producing Saccharomyces cerevisiae strains isolated from coconut toddy. J. Nat. Sci. Found. Sri Lanka. 26, 77–91.
Wu, T.Y., Mohammad, A.W., Jahim, J.M., Anuar, N., 2010. Pollution control technologies for the treatment of palm oil mill effluent (POME) through end-of-pipe processes. J. Environ. Manage. 91 (7), 1467–1490. https://doi.org/10.1016/j.jenvman.2010.02.008.
Xie, W., Ma, N., 2009. Immobilized lipase on Fe3O4 nanoparticles as biocatalyst for biodiesel production. Ener. Fuel. 23, 1347–1353.
Xu, L., Weathers, P.J., Xiong, X.R., Liu, C.Z., 2009. Microalgal bioreactors: challenges and opportunities. Engg. Life. Sci. 9, 178–189.
Yasar, A., Bilgili, M., Yildizhan, S., 2015. The influence of diesel-biodiesel-alcohol blends on the performance and emissions in a diesel engine. Int. J. Sci. Technol. Res. 1, 52–61.
Zaharin, M.S., Abdullah, N.R., Najafi, G., Sharudin, H., Yusaf, T., 2017. Effects of physicochemical properties of biodiesel fuel blends with alcohol on diesel engine performance and exhaust emissions: a review. Renew. Sust. Energ. Rev. 79, 475–493.
Zertuche, L., Zall, R.R., 1985. Optimizing alcohol production from whey using computer technology. Biotechnol. Bioengg. 27 (4), 547–554.